AGU PUBLICATIONS

JGR

Journal of Geophysical Research: Space Physics

RESEARCH ARTICLE
10.1002/2015JA022201

Key Points:
- Polarization electric fields in TIDs are identified
- Quantitative relationship between ion density and ion velocity is derived
- Polarization electric field exists during daytime

Correspondence to:
C.-S. Huang,
chaosong.huang.1@us.af.mil

Citation:
Huang, C.-S. (2016), Plasma drifts and polarization electric fields associated with TID-like disturbances in the low-latitude ionosphere: C/NOFS observations, *J. Geophys. Res. Space Physics*, *121*, 1802–1812, doi:10.1002/2015JA022201.

Received 23 NOV 2015
Accepted 6 JAN 2016
Accepted article online 13 JAN 2016
Published online 27 FEB 2016

©Published 2016. This article is a US Government work and is in the public domain in the United States of America.

Plasma drifts and polarization electric fields associated with TID-like disturbances in the low-latitude ionosphere: C/NOFS observations

Chao-Song Huang[1]

[1]Air Force Research Laboratory, Kirtland AFB, New Mexico, USA

Abstract Medium-scale traveling ionospheric disturbances are often observed at the magnetically conjugate points in the nighttime midlatitude ionosphere. It has been suggested that gravity waves disturb the ionosphere and induce electric fields in one hemisphere and that the electric fields are amplified by the Perkins instability and transmitted along the geomagnetic field lines to the conjugate ionosphere, creating similar disturbances there. However, direct observations of electric fields associated with traveling ionospheric disturbances (TIDs) are very few. In this study, we present low-latitude TID-like disturbances observed by the Communication/Navigation Outage Forecasting System (C/NOFS) satellite. It is found that ion velocity perturbations are generated in the directions parallel and perpendicular to the geomagnetic field within TIDs. Both the parallel and perpendicular ion velocity perturbations show an in-phase correlation with the ion density perturbations. For nighttime TIDs, the amplitude of both the parallel and meridional ion velocity perturbations increases almost linearly with the amplitude of the ion density perturbations, and the meridional ion drift is proportional to the parallel ion velocity. For daytime TIDs, the parallel ion velocity perturbation increases with the ion density perturbation, but the meridional ion velocity perturbation does not change much. The observations provide evidence that polarization electric field is generated within TIDs at low latitudes and maps along the geomagnetic field lines over a large distance.

1. Introduction

A common feature of the ionospheric *F* region is the presence of traveling ionospheric disturbances (TIDs). *Hines* [1960] first recognized the similarities between certain TID properties and the features of atmospheric gravity waves. *Hooke* [1968] analyzed the ionospheric response to the passage of gravity waves and developed the theoretical framework of TIDs. Medium-scale TIDs (MSTIDs) are often observed in the nighttime midlatitude ionosphere [e.g., *Shiokawa et al*., 2003a, 2003b]. The typical wavelength and period of the MSTIDs are 100–300 km and 0.5–1.5 h, respectively. MSTIDs are not limited in a local area. *Otsuka et al*. [2004] found that very symmetric patterns of nighttime MSTIDs occurred simultaneously at Sata, Japan, and Darwin, Australia. When the images of the MSTID in the southern hemisphere are mapped to the conjugate points along the geomagnetic field lines, they coincide perfectly with the images in the Northern Hemisphere. *Shiokawa et al*. [2005] analyzed multiple conjugate events and identified the correspondence of the MSTID structures between the Northern Hemisphere and Southern Hemisphere with comparable amplitudes.

Otsuka et al. [2004] and *Shiokawa et al*. [2005] suggested that the simultaneous occurrence of nighttime MSTIDs at conjugate points is the result of electrodynamic coupling between the two hemispheres along the geomagnetic field lines. Polarization electric field is generated in association with the TIDs in one hemisphere and transmitted along the geomagnetic field lines to the conjugate ionosphere without attenuation because the field lines are almost equipotential, creating similar disturbances in the conjugate hemisphere. *Shiokawa et al*. [2003a] modeled MSTIDs and found that an oscillating electric field of 1.2 mV/m was sufficient to reproduce the observed airglow amplitudes.

The Perkins instability [*Perkins*, 1973] is the possible mechanism responsible for the generation of electric fields in MSTIDs [*Otsuka et al*., 2004; *Shiokawa et al*., 2005]. *Huang et al*. [1994] analyzed the effect of gravity waves in seeding Perkins instability and showed that polarization electric field can be generated by gravity waves at middle latitudes. *Miller* [1997] developed a model in which gravity waves disturb the ionospheric conductivity and the variations in the ionospheric conductivity create divergences in the global current which produce local electric fields. The electric fields are further amplified by the Perkins instability and produce ionospheric disturbances such as turbulent upwelling [*Fukao and Kelley*, 1991].

Conjugate occurrence of electric field perturbations has been observed in the nighttime midlatitude ionosphere. *Saito et al*. [1995, 1998] identified electric field perturbations with a characteristic wavelength of 10–50 km. These electric field perturbations occurred poleward of the equatorial anomaly crests and were not related to equatorial plasma bubbles. Although the characteristic wavelength of the electric field perturbations observed by *Saito et al*. [1995, 1998] is much smaller than the wavelength (typically several hundreds of kilometers) of MSTIDs [*Otsuka et al*., 2004; *Shiokawa et al*., 2003a, 2003b, 2005], the observations of *Saito et al*. [1995, 1998] have been used as evidence of the polarization electric field that produces conjugate MSTIDs. *Shiokawa et al*. [2003b] identified a one-to-one correspondence between the electric field perturbations detected by the Defense Meteorological Satellite Program satellite and the MSTID wave structures observed by a ground airglow imager and suggested that the electric field is polarization field.

Numerical simulations have been used to study the occurrence of MSTIDs. *Krall et al*. [2011] used a traveling wave electric field with vertical $\mathbf{E}\times\mathbf{B}$ drifts of up to $\pm 50\,\mathrm{m\,s^{-1}}$ as input to the SAMI3 ionospheric model and found that the localized model $\mathbf{E}\times\mathbf{B}$ drifts cause disturbances of nonlocal ionospheric potential and produce a faint MSTID-like plasma density wave in the conjugate ionosphere. The simulations of *Duly et al*. [2014] show that a random perturbation can result in the development of nighttime MSTIDs at midlatitudes. Electric fields are generated within the developed MSTIDs, although the amplitude of the electric field perturbations in the simulations is small compared to experimental observations. *Huba et al*. [2015] simulated ionospheric effects associated with tsunami-driven gravity waves. The simulation results show that plasma velocity/electric field perturbations are generated in the gravity wave-induced variations. In particular, electric field induced by the gravity waves in one hemisphere is transmitted to the conjugate hemisphere.

Polarization electric field is used to explain the conjugate occurrence of the MSTIDs [*Otsuka et al*., 2004; *Shiokawa et al*., 2005]. However, direct observations of plasma velocities/electric fields associated with nighttime MSTIDs are very few [*Saito et al*., 1995, 1998; *Shiokawa et al*., 2005]. These observed electric fields, corresponding to plasma drifts of several tens of meters per second perpendicular to the magnetic field, are assumed to have been amplified by the Perkins instability. In contrast, the $\mathbf{E}\times\mathbf{B}$ drifts generated within gravity wave-induced perturbations at low latitudes, without involving the Perkins instability, in numerical simulations are only a few meter per second [*Huba et al*., 2015].

In this study, we analyze TID-like disturbances in ion density and ion velocity measured by the Communication/Navigation Outage Forecasting System (C/NOFS) satellite at low latitudes. Our objectives are to identify the occurrence of plasma drifts/electric fields within TID-like disturbances, to determine whether the Perkins instability is involved in large plasma drifts, to examine whether polarization electric fields can exist during daytime besides nighttime, and to derive quantitative relationships between the ion density and velocity perturbations.

2. Observations

We select several cases in which quasiperiodic disturbances occur in the ion density and ion velocity for this study. The ion density and ion velocity were measured by the ion velocity meter (IVM) on board C/NOFS. The vector electric field instrument (VEFI) on board C/NOFS measures electric field that can be converted into $\mathbf{E}\times\mathbf{B}$ drift velocities. We will analyze ion velocities both perpendicular and parallel to the geomagnetic fields. IVM has measurements of parallel and perpendicular ion velocities, and the $\mathbf{E}\times\mathbf{B}$ drift velocities derived from VEFI measurements are in the directions perpendicular to the magnetic field. Therefore, we choose IVM data for this study. C/NOFS has a low-inclination (±13° geographic latitude) orbit, with an orbital period of ~100 min. Because of the offset between the geographic and geomagnetic latitudes, C/NOFS can be ±25° away from the geomagnetic equator in some longitude regions.

We will analyze quasiperiodic disturbances during both daytime and nighttime. For nighttime disturbances, a closely related phenomenon is equatorial plasma bubble. There have been many reports of plasma bubbles observed by C/NOFS. A typical feature of plasma bubbles is the existence of large upward ion drifts inside the depleted density region [e.g., *Huang et al*., 2011, 2012; *Huang and Hairston*, 2015]. Here we present two examples of isolated plasma bubbles to show the anticorrelation between the ion density and the ion vertical drift inside the bubble.

Figures 1a–1d show a plasma bubble in the evening sector. In Figure 1a, the black line represents the magnetic equator, the red line represents the latitude of C/NOFS, and the dashed blue line, labeled on the right,

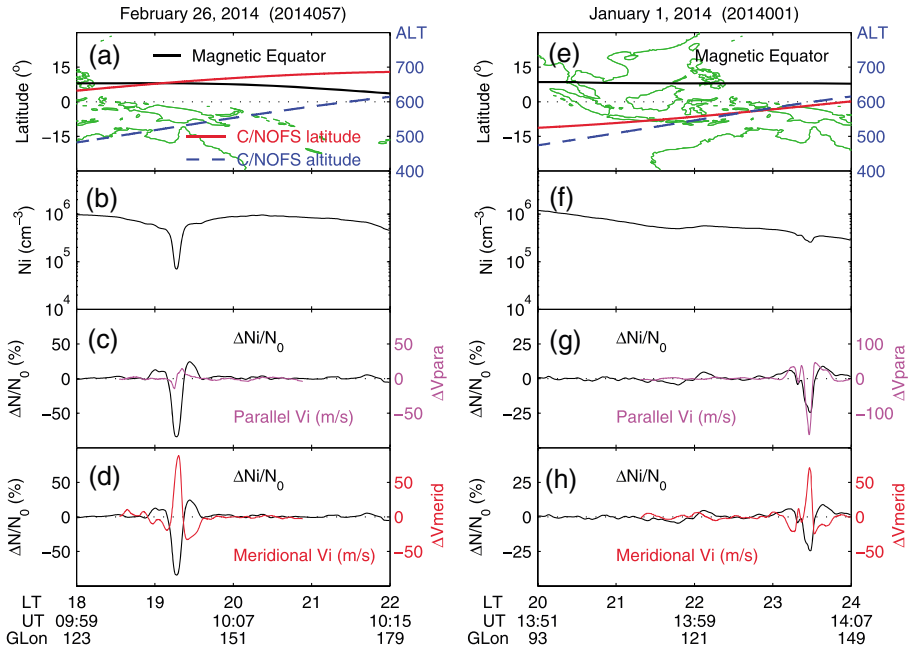

Figure 1. Examples of plasma drifts associated with equatorial plasma bubbles observed by the C/NOFS satellite. (a–d) The case on 26 February 2014. In Figure 1a, the black line represents the magnetic equator, the red line represents the latitude of C/NOFS, and the dashed blue line, labeled on the right, represents the altitude (in kilometers) of C/NOFS, respectively. Figure 1b shows the ion density. In Figures 1c and 1d, the black line represents the relative perturbation of the ion density, the magenta line in Figure 1c represents the perturbation of the ion velocity component parallel to the magnetic field, and the red line in Figure 1d represent the perturbation of the ion velocity component perpendicular to the magnetic field. (e–h) The case that occurred on 1 January 2014.

represents the altitude (in kilometers) of C/NOFS, respectively. In general, plasma bubbles are identified from the change of the ion density and ion velocity. Figure 1b shows the ion density. Since this study focuses on the perturbations of the ion density and ion velocity in order to identify TID-like disturbances, we also plot the perturbations for the cases of plasma bubbles. The average value of the ion density and ion velocity is calculated over 140 s, corresponding to a longitudinal coverage of ~1000 km. The black line in Figures 1c and 1d represents the relative density perturbation ($\Delta N_i/N_0$). For the parallel and meridional ion velocities, we simply remove the average value, so the magenta and red lines in Figures 1c and 1d represent the velocity perturbations. In IVM data, the meridional component of the ion drift velocity is defined to be in the direction perpendicular to the magnetic field lines in the meridian plane. Near the magnetic equator, the magnetic field lines are almost horizontal, so the meridional component of the ion drift velocity is very close to the vertical component.

A plasma bubble was detected at ~1915 LT when C/NOFS was almost exactly over the magnetic equator in the case of 26 February 2014. The ion density inside the bubble was decreased by an order of magnitude, and the meridional ion drift was increased by ~100 m s^{-1} over the background ion drift. The perturbation of the parallel ion velocity was relatively small, perhaps because C/NOFS was at the magnetic equator. In the case of 1 January 2014 (Figures 1e–1h), a relatively weak plasma bubble was detected near midnight when C/NOFS was ~10° away from the magnetic equator. The meridional ion drift was also enhanced inside the bubble. The parallel ion velocity was quite large in this case, which may represent the fact that the parallel ion velocity was accelerated by the gravity and the parallel electric field inside the bubble. Plasma bubbles are not a new phenomenon and not analyzed in detail here. The ion density and velocity perturbations of plasma bubbles in Figure 1 are plotted for comparing with TID-like disturbances.

We now start to study nighttime TID-like disturbances. Figures 2a–2d present a case in which quasiperiodic disturbances were detected during nighttime when C/NOFS was close to the magnetic equator. Perturbations in the background ion density in Figure 2b are not obvious. In contrast, quasiperiodic disturbances can be identified in the relative density perturbations (the black line in Figures 2c and 2d). C/NOFS took 23 min to

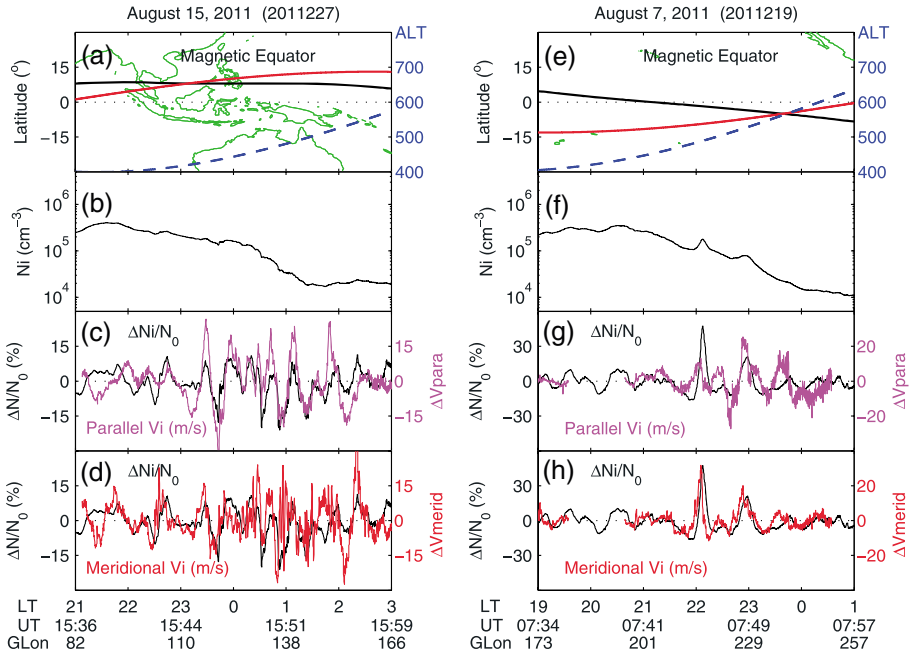

Figure 2. TID-like disturbances observed by C/NOFS near the magnetic equator during nighttime.

fly over the plotted longitudinal range of 84°. It is reasonable to assume that the plasma disturbances did not move significantly within this interval. The measured disturbances represent spatial structures rather than temporal variations. We use the separation between two successive wave peaks along the C/NOFS track to characterize the apparent wavelength of the plasma disturbances. Because C/NOFS only made one-dimensional measurements along its track, we cannot determine the wavefront and the wavelength perpendicular to the wavefront. The apparent wavelength between 2300 and 0300 LT is ~650 km, the amplitude of the relative density perturbations is ~10%, the amplitude of the parallel ion velocity perturbations is ~20 m s^{-1}, and the amplitude of the meridional ion velocity perturbations is also ~20 m s^{-1}. The plasma disturbances in Figures 2e and 2f show similar amplitudes but longer apparent wavelength of ~1000 km.

Because the satellite track may not be exactly perpendicular to the wavefront of the plasma disturbances, the wavelength of the disturbances in the direction of wave propagation is shorter than the measured apparent wavelength. For example, if we assume that the plasma disturbances propagate in the southwest direction (45° off the equator), the wavelength perpendicular to the wavefront is ~0.7 times the apparent wavelength along the equator, so the wavelength of the plasma disturbances might be ~460 km in this case if the disturbances indeed propagated at an angle of 45° to the equator. The period of the plasma disturbances cannot be determined from the satellite measurements but can be derived from radar measurements. In a case with radar data which will be shown later, the period of similar plasma disturbances is ~1.5 h.

An important feature of the plasma disturbances is that both the parallel and meridional ion velocities show in-phase correlation with the ion density perturbations. When the ion density is increased, the ion velocities are enhanced, and verse vice. This in-phase correlation between the velocity and density perturbations is consistent with the TID theory [*Hooke*, 1968]. This feature is very different from plasma bubbles. Plasma bubbles may be also quasiperiodic [*Huang et al.*, 2013], but, in general, large vertical ion drifts occur in the depleted density region. Plasma density enhancements with large vertical ion drifts may be associated with plasma bubbles [*Huang et al.*, 2014b]. In this study, we specifically selected the cases in August, typically a season with low occurrence probability of plasma bubbles [*Huang et al.*, 2014a]. We also checked C/NOFS data during the previous and following orbits to make sure that no plasma bubbles existed at these longitudes. The plasma disturbances presented in Figure 2 and below are not related to plasma bubbles. The wavelength and period of the quasiperiodic plasma disturbances in the C/NOFS measurements are similar to the nighttime MSTIDs [*Shiokawa et al.*, 2003a, 2003b], although the C/NOFS measurements are made at lower latitudes. Therefore, the plasma disturbances in this study are termed TID-like disturbances.

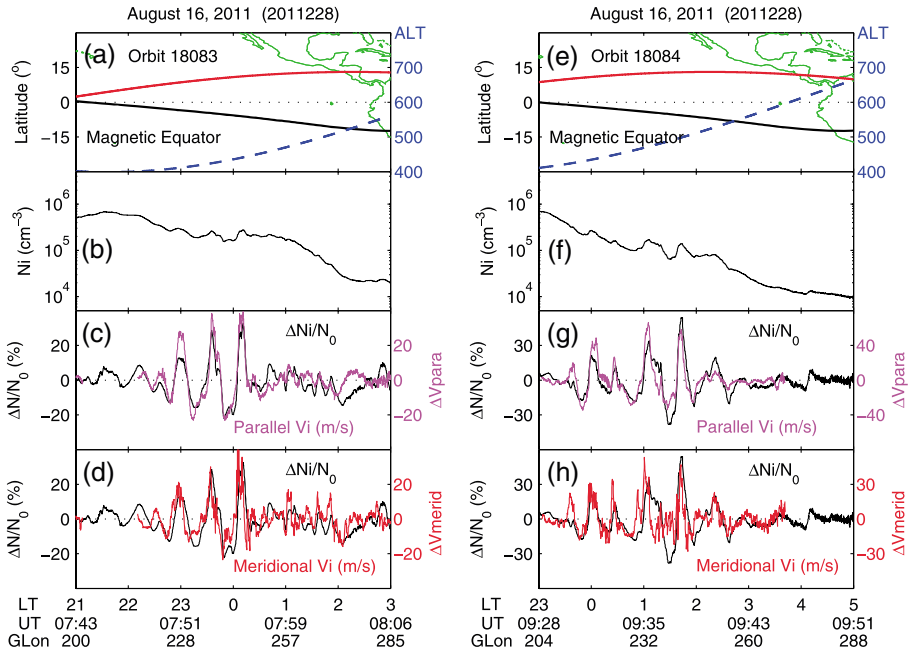

Figure 3. TID-like disturbances observed by C/NOFS off the magnetic equator during nighttime on 16 August 2011.

Figure 3 presents nighttime TID-like disturbances measured by C/NOFS when C/NOFS was off the magnetic equator by 10–20° over two successive orbits on 16 August 2011. Both the parallel and meridional components of the ion velocity perturbations coincided extremely well with the ion density perturbations. The perturbations of the ion density and ion velocity were intensifying toward later times. Different scales are used in Figures 3c–3d and 3g–3h. During Orbit 18084 (Figures 3e–3h), the amplitude of the ion density perturbations reaches ~30%, and the amplitude of both velocity components reaches 30–40 m s^{-1}. The apparent wavelength of the disturbances along the C/NOFS track is ~800 km.

The shape of the ion density and velocity perturbations are very similar in Figures 3a–3d and 3e–3h. It appears that the same disturbances were detected by C/NOFS over the two orbits. This is indeed the case. We plot the ion density and the density perturbations during the two orbits in Figure 4 for comparison. In Figures 4a and 4b, the data are plotted at the longitudes where they were measured. In Figures 4c and 4d,

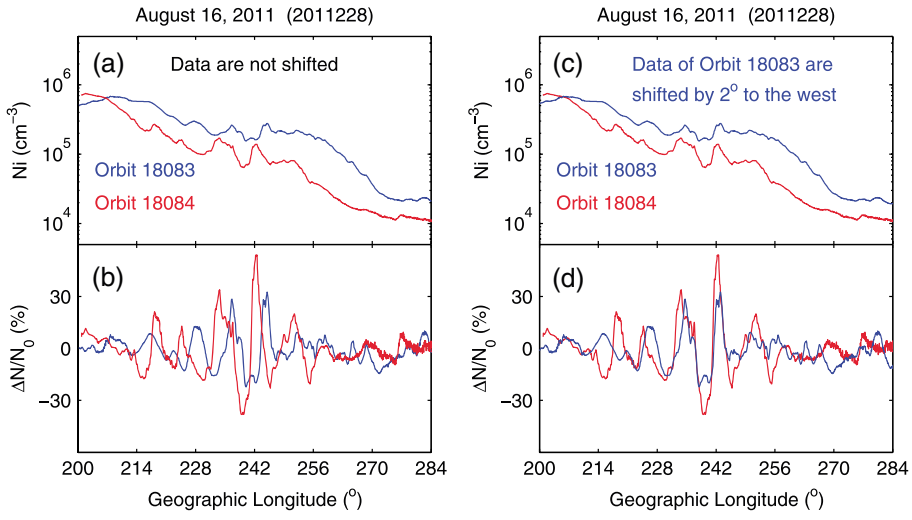

Figure 4. The ion density and relative density perturbations measured by C/NOFS during two successive orbits on 16 August 2011.

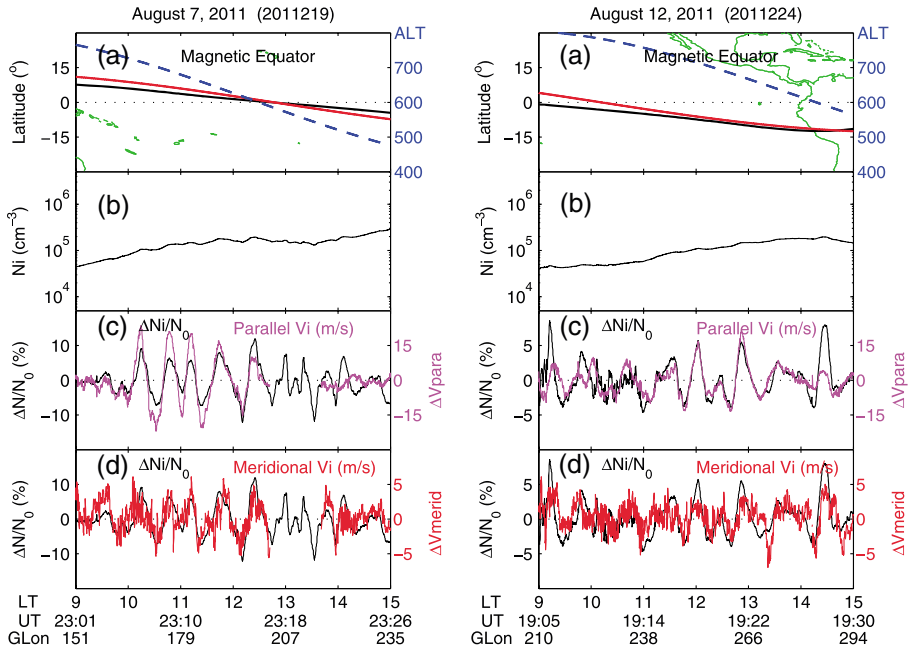

Figure 5. TID-like disturbances observed by C/NOFS near the magnetic equator during daytime.

the data during Orbit 18083 are shifted by 2° in longitude to the west. Then the large density perturbations between 220° and 256° coincide very well during the two orbits. This means that the plasma disturbances traveled by ~2° westward over the two orbits. If we take the density perturbation peaks at ~242° in Figure 2d to calculate the propagation speed, this speed is ~50 m s^{-1} in the westward direction. The propagation direction and speed of the plasma disturbances are also similar to the nighttime MSTIDs [*Shiokawa et al.*, 2003a, 2003b]. It should be mentioned that the propagation speed of ~50 m s^{-1} is calculated along the C/NOFS track. If the C/NOFS track was not perpendicular to the wavefront of the plasma disturbances, the real propagation speed of the plasma disturbances could be smaller.

TID-like disturbances are detected by C/NOFS not only at night but also during daytime. Figure 5 shows the daytime plasma disturbances in two cases when C/NOFS flew almost exactly along the magnetic equator. In these cases, the apparent wavelength of the plasma disturbances is ~800 km, the amplitude of the ion density perturbations is 5–10%, the amplitude of the parallel ion velocity perturbations is ~15 m s^{-1}, and the amplitude of the meridional ion velocity perturbations is ~5 m s^{-1}. An important phenomenon is that ion velocity perturbations perpendicular to the geomagnetic field occur during daytime.

Figure 6 presents additional two cases of daytime TID-like disturbances. In the case of 3 August 2011 (Figures 6a–6d), four cycles of plasma disturbances were detected between 1100 and 1300 LT when C/NOFS flew nearly along the magnetic equator. In the case of 1 August 2011 (Figures 6e–6h), C/NOFS was 15–20° away from the magnetic equator and detected quasiperiodic disturbances in the ion density and ion velocity. The apparent wavelength of the plasma disturbances is ~600 km in the case of 3 August and ~800 km in the case of 1 August, respectively. The amplitudes of the ion density and ion velocity perturbations are similar to those in Figure 5.

The meridional ion velocity in the daytime TID-like disturbances in Figures 5 and 6 is not large but indeed occurs. We present an example in which similar velocity perturbations were measured simultaneously by the C/NOFS satellite and by the Jicamarca incoherent scatter radar. Figures 7a–7d show the plasma disturbances measured by C/NOFS when it was ~20° away from the magnetic equator on 8 June 2011. C/NOFS detected quasiperiodic disturbances and passed the Jicamarca longitude (284°) at 1839 LT. The amplitude of the meridional ion velocity perturbations measured by C/NOFS is ~5 m s^{-1}. The Jicamarca radar measurements are presented in Figures 7e and 7f. Figure 7e shows the vertical ion drift measured by the radar, and Figure 7f shows the velocity perturbations after the average value is removed. The velocity perturbation in the radar data is also ~5 m s^{-1} at ~1900 LT, very consistent with the satellite measurements. The ion drift

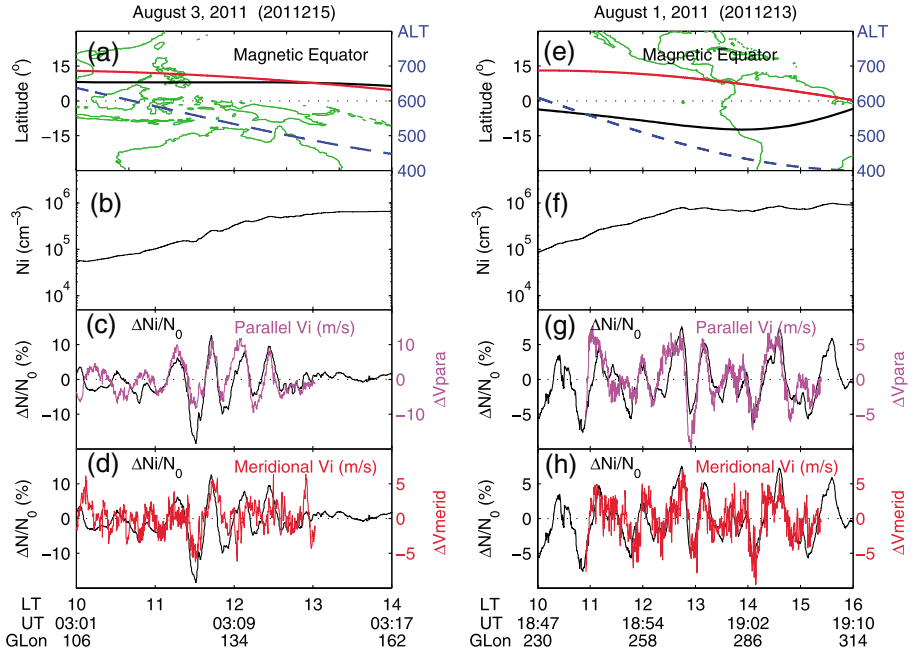

Figure 6. TID-like disturbances observed by C/NOFS off the magnetic equator during daytime.

velocity from the measurement of the Jicamarca radar is determined primarily by the contribution near the *F* peak, which could be lower than the altitude of the C/NOFS measurements. The apparent wavelength of the plasma disturbances is ~800 km, from the C/NOFS data, and the period of the plasma disturbances is ~1.5 h, from the radar data. The period of ~1.5 h is measured only in this case. Another important fact is that the similar meridional/vertical ion drifts are measured simultaneously at different latitudes. The Jicamarca radar is located almost at the magnetic equator, and C/NOFS was at ~20° away from the magnetic equator when it

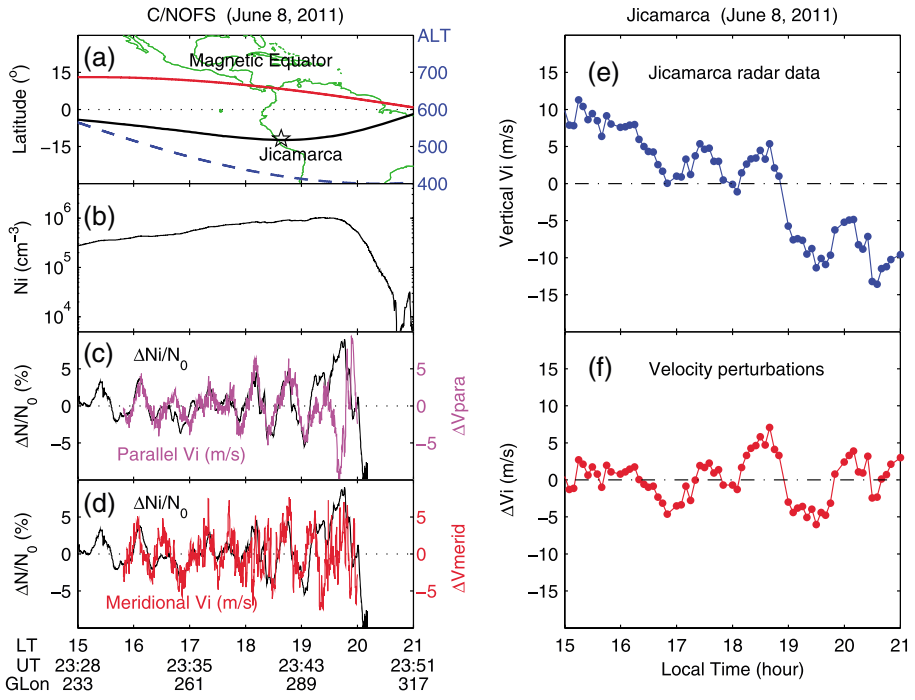

Figure 7. TID-like disturbances measured nearly simultaneously by the C/NOFS satellite and by the Jicamarca incoherent scatter radar during daytime on 8 June 2011.

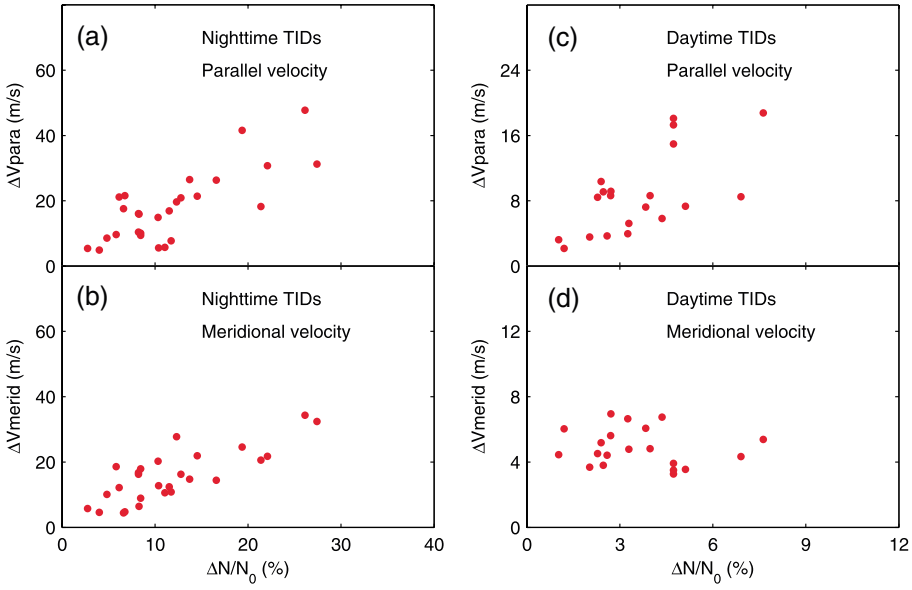

Figure 8. Relationship between the ion density and ion velocity perturbations in TID-like disturbances.

passed the longitude of Jicamarca. The simultaneous measurements of similar ion drifts at two locations separated by 20° in latitude indicate that the ionospheric electric field can be indeed transmitted along the geomagnetic field lines over a large distance.

It can be clearly seen that the ion velocities, both the parallel and meridional components, coincide very well with the ion density perturbations in all cases presented in Figures 2–7. This implies that the ion velocity perturbation is correlated with, or proportional to, the ion density perturbation. We can demonstrate this relationship by plotting the velocity perturbation as a function of the density perturbation. We use the data from the cases of Figures 2–7 to calculate the ion density and velocity perturbations. The amplitude of the ion density or velocity perturbation, ΔV or $\Delta N/N_0$, is defined to be half the valley-to-peak variation. Figures 8a and 8b show the result of the nighttime disturbances, and Figures 8c and 8d show the result of the daytime disturbances. In Figures 8a and 8b, the nighttime parallel or meridional ion velocity perturbation increases approximately linearly with the density perturbation. In Figure 8c, the daytime parallel velocity perturbation also increases with the density perturbation. However, the daytime meridional velocity perturbation is ~5 m s^{-1} and does not change much with the density perturbation (Figure 8d). Figure 9 shows the relationship between the parallel and meridional ion velocity perturbations. The nighttime meridional ion velocity increases with the parallel velocity (Figure 9a). In contrast, the daytime meridional ion velocity remains near 5 m s^{-1} although the parallel velocity varies from 2 to 20 m s^{-1} (Figure 9b).

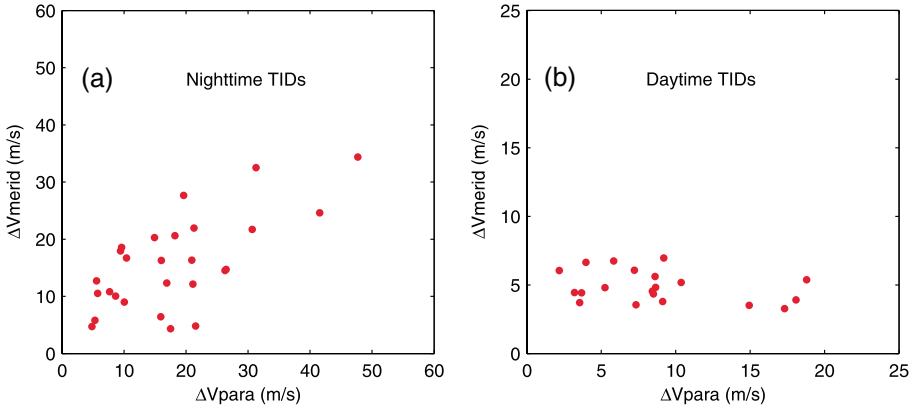

Figure 9. Relationship between the parallel and meridional ion velocity perturbations in TID-like disturbances.

3. Discussion

Figures 2–9 present C/NOFS measurements of quasiperiodic ionospheric disturbances. A prominent feature of these disturbances is that the perturbations of the parallel and meridional ion velocities are well correlated with the ion density perturbations. In fact, the amplitude of the ion velocity perturbations is almost linearly proportional to the amplitude of the ion density perturbations. According to the theory of *Hooke* [1968], a linear relationship exists between the ion density and ion parallel velocity perturbations for TIDs. Our observations are consistent with this theory. In one of our cases, the ionospheric disturbances traveled westward with a speed of ~50 m s^{-1}. This is consistent with the typical southwest propagation of MSTIDs at midlatitudes [*Shiokawa et al*., 2003a, 2003b], although the plasma disturbances in our cases were observed near the magnetic equator. The apparent wavelength of the plasma disturbances along the satellite track is 600–850 km. If we assume that the plasma disturbances propagated at an angle of 45° relative to the magnetic equator, the wavelength perpendicular to the wavefront would be 400–600 km. This wavelength is larger than that of the midlatitude MSTIDs [*Shiokawa et al*., 2003a, 2003b] but is still in the range of medium-scale TIDs. Large-scale TIDs often mean those with wavelength of $>$1000 km.

On the other hand, the local theory of *Hooke* [1968] and *Huang et al*. [1994] suggests that a polarization electric field perpendicular to the geomagnetic field is hardly generated by TIDs unless the TIDs propagate exactly perpendicular to the geomagnetic field. However, as addressed by *Miller* [1997], the local theory does not consider the variations of the ionospheric conductivity caused by gravity waves. When the conductivity variations are included, polarization electric field will occur. The numerical simulations of *Huba et al*. [2015] show that polarization electric field is indeed generated by tsunami-driven gravity waves. The gravity waves cause plasma velocity variations both perpendicular and parallel to the geomagnetic field, and the polarization electric field is transmitted to the magnetically conjugate region.

Other electrodynamic processes can also produce quasiperiodic plasma disturbances in the equatorial ionosphere. *Huang et al*. [2013] reported quasiperiodic plasma bubbles that have a characteristic longitudinal separation of 500–800 km. However, the plasma disturbances presented in this paper are not plasma bubbles or plasma density enhancements associated with plasma bubbles [*Huang et al*., 2014b]. As shown in Figures 8 and 9, the ion velocity perturbation is proportional to the ion density perturbation, and the parallel ion velocity perturbation is proportional to the meridional ion velocity perturbation. No theory of plasma bubbles has predicted such relationships. In addition, we checked C/NOFS data during the orbits immediately before and after the quasiperiodic disturbances and did not see any existence of plasma bubbles. Therefore, the quasiperiodic plasma disturbances are explained to be TIDs.

In Figure 8a, the parallel ion velocity perturbation increases linearly with the ion density perturbation. Although such a relationship was predicted for TIDs several decades ago [e.g., *Hooke*, 1968], observational verifications are seldom available. Furthermore, as shown in Figures 8b and 9a, the meridional ion velocity perturbation increases linearly with the ion density perturbation and with the parallel ion velocity perturbation. To the best of our knowledge, these quantitative relationships are observed for the first time.

The proportionality of the meridional ion velocity perturbation with the parallel ion velocity perturbation is an interesting phenomenon. In the model of *Miller* [1997], gravity waves induce perturbations in ionospheric conductivity, the perturbations in ionospheric conductivity cause local electric field perturbations to develop, and all gravity waves which produce observable TIDs may produce ionospheric electric fields. On the basis of this theory, we may assume that gravity waves with larger amplitude cause larger perturbations in ionospheric conductivity, resulting in the generation of larger electric field/plasma drift. Our study provides support for the theory of *Miller* [1997]. According to the theory of *Hooke* [1968], the parallel ion velocity associated with TIDs is caused primarily by the component of the neutral velocity along the geomagnetic field lines. Gravity waves with larger amplitude cause larger parallel ion velocity and larger meridional ion drift/zonal polarization electric field through the variation in the ionospheric conductivity. As a result, the meridional ion drift is approximately proportional to the parallel ion velocity in the TIDs.

The nighttime meridional ion drift, which is perpendicular to the geomagnetic field, reaches a maximum value of ~30 m s^{-1} in our observations, corresponding to an eastward electric field of 0.75 mV/m if we take a mean value of 2.5×10^4 nT for the magnetic field in the equatorial ionosphere. In the cases of *Saito et al*. [1995, 1998] and *Shiokawa et al*. [2003b], the electric field perturbations were ~1 mV/m. The maximum ion

drift/electric field in our cases is close to their studies. However, *Saito et al*. [1995, 1998] and *Shiokawa et al*. [2003b] assumed that the observed electric field was not the gravity wave-induced electric field but the electric field that was amplified by the Perkins instability at midlatitudes. In the numerical simulations of *Huba et al*. [2015], gravity waves are assumed to occur at 18–20° magnetic latitudes, and the maximum meridional ion drift is only a few meters per second, perhaps without involvement of the Perkins instability.

In our cases, the ion drifts were observed near the magnetic equator. If any plasma instability is involved, it should be the Rayleigh-Taylor instability, rather than the Perkins instability. The maximum meridional ion drift in the nighttime TIDs of our observations is much larger than that in the simulations of *Huba et al*. [2015]. Although we concluded that the plasma disturbances in our cases are not plasma bubbles, we cannot exclude the possibility that the Rayleigh-Taylor instability could have played a role in amplifying the gravity wave-induced electric field. The amplitude of the ion density perturbations in the nighttime TIDs reaches ~30%, and some nonlinear processes may have taken effect. In addition, the meridional plasma drift (polarization electric field) of the nighttime TIDs is larger than that of the daytime TIDs, and the existence of the Rayleigh-Taylor instability in the nighttime equatorial ionosphere could contribute to this difference.

The daytime ion velocity perturbations show very different features. In Figure 8c, the parallel ion velocity perturbation is approximately proportional to the ion density perturbation. This relationship between the ion density and parallel ion velocity is consistent with the TID theory [*Hooke*, 1968]. The unusual feature is that meridional ion drifts associated with TIDs are observed during daytime. The daytime meridional ion drifts are, in general, much smaller than the corresponding nighttime drifts and appear to be saturated at a level of ~5 m s^{-1}. The primary cause for the smaller daytime drifts may be the existence of high-conducting *E* layers in both hemispheres, shorting out the polarization electric field associated with TIDs. On the other hand, the occurrence of the daytime meridional ion drifts implies that the shorting out effect of the *E* layers is not perfect.

MSTIDs have been frequently observed in the nighttime midlatitude ionosphere [*Shiokawa et al*., 2003a, 2003b, 2005], and polarization electric field and its mapping along the geomagnetic field lines are used to explain the occurrence of similar structures at the conjugate points in two hemispheres. The midlatitude nighttime electric field is assumed to be amplified by the Perkins instability [*Saito et al*., 1995, 1998; *Otsuka et al*., 2004; *Shiokawa et al*., 2005]. Our observations show that polarization electric field occurs in TIDs at low latitudes. The nighttime polarization electric field at low latitudes is comparable to the midlatitude electric field but without involvement of the Perkins instability. We have also found that similar meridional ion drifts (or zonal polarization electric fields) are measured nearly simultaneously by the C/NOFS satellite and by the Jicamarca incoherent scatter radar. Our observations provide further support for the scenario that polarization electric field exists along the magnetic field lines.

In this study, we concentrate on the analysis of the ion density and ion velocity perturbations. It is generally believed that TIDs, including the midlatitude MSTIDs, are induced by atmospheric gravity waves. A potential source of gravity waves at low latitudes is mesoscale convective system in the troposphere. These mesoscale convective systems are usually within the intertropical convergence zone [*Waliser and Gautier*, 1993]. Gravity waves generated by the mesoscale convective systems propagate up to the *F* region and induce perturbations in plasma density [*Tsunoda*, 2010]. Gravity waves at middle latitudes [*Shiokawa et al*., 2003a, 2003b] can propagate to low latitudes and cause plasma disturbances there. However, we have not investigated where the gravity waves in our cases originate, why the wavelength and period of the TIDs/gravity waves are those as observed, how frequently such TID-like disturbances occur in the equatorial ionosphere, whether polarization electric field occurs in all TIDs, etc. These issues will be explored in the future.

4. Conclusions

We have presented C/NOFS measurements of quasiperiodic ionospheric disturbances in several cases and specifically examined the ion velocity perturbations. These events were selected from a season with low occurrence of plasma bubbles. We also checked the C/NOFS orbits immediately before and after the selected data range to make sure that no plasma bubbles were associated with the quasiperiodic ionospheric disturbances we are interested here. The major conclusions are as follows.

Quasiperiodic disturbances of the ion density and ion velocity occur in the low-latitude ionosphere. The apparent wavelength of the plasma disturbances along the satellite track, approximately along the equator, is 600–850 km,

and a westward traveling speed of ~50 m s^{-1} is derived in one case. The plasma disturbances show a period of ~ 1.5 h that is observed by the Jicamarca incoherent scatter radar. The quasiperiodic plasma disturbances occur during both daytime and nighttime and are identified as TIDs or TID-like disturbances.

Both the parallel and meridional ion velocity perturbations show an in-phase correlation with the ion density perturbations in the TID-like disturbances. For nighttime TIDs, both the parallel and meridional ion velocity perturbations are approximately proportional to the ion density perturbation, and a linear relationship exists between the parallel and meridional ion velocity perturbations. The nighttime parallel ion velocity perturbations can reach 50 m s^{-1}, and the nighttime meridional ion velocity perturbations can reach 30 m s^{-1}. For daytime TIDs, only the parallel ion velocity perturbation is approximately proportional to the ion density perturbation, and the meridional ion drift remains at the level of ~5 m s^{-1}.

The meridional ion drift of 30 m s^{-1} corresponds to a zonal polarization electric field of ~0.75 mV/m. The observations show that polarization electric field can be generated in nighttime TIDs in the equatorial ionosphere. The existence of the meridional ion drift of ~5 m s^{-1} in daytime TIDs suggests that the polarization electric field in the *F* region is not completely shorted out by the *E* layers. Similar meridional ion drifts are observed simultaneously at the magnetic equator and ~20° away from the magnetic equator at the same longitude, indicating that polarization electric field can be transmitted along the geomagnetic field lines over a large distance.

Acknowledgments

The C/NOFS mission is supported by the Air Force Research Laboratory, the SMC Defense Weather Systems Directorate, the Department of Defense Space Test Program, the National Aeronautics and Space Administration, the Naval Research Laboratory, and The Aerospace Corporation. Work at the Air Force Research Laboratory was supported in part by NASA grant NNH15AZ81I. CINDI data are provided through the auspices of the CINDI team at the University of Texas at Dallas supported by NASA grant NAS5-01068. C/NOFS data are available in the NASA database (http://cdaweb.gsfc.nasa.gov/istp_public/). The Jicamarca Radio Observatory is a facility of the Instituto Geofisico del Peru operated with support from the NSF AGS-1433968 through Cornell University.

References

Duly, T. M., J. D. Huba, and J. J. Makela (2014), Self-consistent generation of MSTIDs within the SAMI3 numerical model, *J. Geophys. Res. Space Physics*, *119*, 6745–6757, doi:10.1002/2014JA020146.

Fukao, S., and M. C. Kelley (1991), Turbulent upwelling of the midlatitude ionosphere: 1. Observational results by the MU radar, *J. Geophys. Res.*, *96*, 3725–3746, doi:10.1029/90JA02253.

Hines, C. O. (1960), Internal atmospheric gravity waves at ionospheric heights, *Can. J. Phys.*, *38*, 1441–1481.

Hooke, W. H. (1968), Ionospheric irregularities produced by internal atmospheric gravity waves, *J. Atmos. Sol. Terr. Phys.*, *30*, 795–823.

Huang, C.-S., and M. R. Hairston (2015), The postsunset vertical plasma drift and its effects on the generation of equatorial plasma bubbles observed by the C/NOFS satellite, *J. Geophys. Res. Space Physics*, *120*, 2263–2275, doi:10.1002/2014JA020735.

Huang, C.-S., C. A. Miller, and M. C. Kelley (1994), Basic properties and gravity wave initiation of the midlatitude *F* region instability, *Radio Sci.*, *29*, 395–405, doi:10.1029/93RS01669.

Huang, C.- S., O. de La Beaujardiere, P. A. Roddy, D. E. Hunton, R. F. Pfaff, C. E. Valladares, and J. O. Ballenthin (2011), Evolution of equatorial ionospheric plasma bubbles and formation of broad plasma depletions measured by the C/NOFS satellite during deep solar minimum, *J. Geophys. Res.*, *116*, A03309, doi:10.1029/2010JA015982.

Huang, C.-S., O. de La Beaujardiere, P. A. Roddy, D. E. Hunton, J. O. Ballenthin, and M. R. Hairston (2012), Generation and characteristics of equatorial plasma bubbles detected by the C/NOFS satellite near the sunset terminator, *J. Geophys. Res.*, *117*, A11313, doi:10.1029/2012JA018163.

Huang, C.-S., O. de La Beaujardiere, P. A. Roddy, D. E. Hunton, J. O. Ballenthin, M. R. Hairston, and R. F. Pfaff (2013), Large-scale quasiperiodic plasma bubbles: C/NOFS observations and causal mechanism, *J. Geophys. Res. Space Physics*, *118*, 3602–3612, doi:10.1002/jgra.50338.

Huang, C.-S., O. de La Beaujardiere, P. A. Roddy, D. E. Hunton, J. Y. Liu, and S. P. Chen (2014a), Occurrence probability and amplitude of equatorial ionospheric irregularities associated with plasma bubbles during low and moderate solar activities (2008–2012), *J. Geophys. Res. Space Physics*, *119*, 1186–1199, doi:10.1002/2013JA019212.

Huang, C.-S., G. Le, O. de La Beaujardiere, P. A. Roddy, D. E. Hunton, R. F. Pfaff, and M. R. Hairston (2014b), Relationship between plasma bubbles and density enhancements: Observations and interpretation, *J. Geophys. Res. Space Physics*, *119*, 1325–1336, doi:10.1002/2013JA019579.

Huba, J. D., D. P. Drob, T.-W. Wu, and J. J. Makela (2015), Modeling the ionospheric impact of tsunami-driven gravity waves with SAMI3: Conjugate effects, *Geophys. Res. Lett.*, *42*, 5719–5726, doi:10.1002/2015GL064871.

Krall, J., J. D. Huba, S. L. Ossakow, G. Joyce, J. J. Makela, E. S. Miller, and M. C. Kelley (2011), Modeling of equatorial plasma bubbles triggered by non-equatorial traveling ionospheric disturbances, *Geophys. Res. Lett.*, *38*, L08103, doi:10.1029/2011GL046890.

Miller, C. A. (1997), Electrodynamics of midlatitude spread *F*: 2. A new theory of gravity wave electric fields, *J. Geophys. Res.*, *102*, 11,533–11,538, doi:10.1029/96JA03840.

Otsuka, Y., K. Shiokawa, T. Ogawa, and P. Wilkinson (2004), Geomagnetic conjugate observations of medium-scale traveling ionospheric disturbances at midlatitude using all-sky airglow imagers, *Geophys. Res. Lett.*, *31*, L15803, doi:10.1029/2004GL020262.

Perkins, F. (1973), Spread *F* and ionospheric currents, *J. Geophys. Res.*, *78*, 218–226, doi:10.1029/JA078i001p00218.

Saito, A., T. Iyemori, M. Sugiura, N. C. Maynard, T. L. Aggson, L. H. Brace, M. Takeda, and M. Yamamoto (1995), Conjugate occurrence of the electric field fluctuations in the nighttime midlatitude ionosphere, *J. Geophys. Res.*, *100*, 21,439–21,452, doi:10.1029/95JA01505.

Saito, A., T. Iyemori, L. G. Blomberg, M. Yamamoto, and M. Takeda (1998), Conjugate observations of the mid-latitude electric field fluctuations with the MU radar and the Freja satellite, *J. Atmos. Sol. Terr. Phys.*, *60*, 129–140.

Shiokawa, K., C. Ihara, Y. Otsuka, and T. Ogawa (2003a), Statistical study of nighttime medium-scale traveling ionospheric disturbances using midlatitude airglow images, *J. Geophys. Res.*, *108*(A1), 1052, doi:10.1029/2002JA009491.

Shiokawa, K., Y. Otsuka, C. Ihara, T. Ogawa, and F. J. Rich (2003b), Ground and satellite observations of nighttime medium-scale traveling ionospheric disturbance at midlatitude, *J. Geophys. Res.*, *108*(A4), 1145, doi:10.1029/2002JA009639.

Shiokawa, K., et al. (2005), Geomagnetic conjugate observation of nighttime medium-scale and large-scale traveling ionospheric disturbances: FRONT3 campaign, *J. Geophys. Res.*, *110*, A05303, doi:10.1029/2004JA010845.

Tsunoda, R. T. (2010), On seeding equatorial spread *F* during solstices, *Geophys. Res. Lett.*, *37*, L05102, doi:10.1029/2010GL042576.

Waliser, D. E., and C. Gautier (1993), A satellite-derived climatology of the ITCZ, *J. Clim.*, *6*(11), 2162, doi:10.1175/1520-0442.